



universität
wien

MASTERARBEIT

Titel der Masterarbeit

Raman-spectroscopic measurements on
UHP microdiamond and diamond abrasives

verfasst von

Claudia Reissner, BSc

angestrebter akademischer Grad

Master of Science (MSc)

Wien, 2015

Studienkennzahl lt. Studienblatt
Studienrichtung lt. Studienblatt
Betreut von:

A 066 815
Masterstudium Erdwissenschaften
Univ.-Prof. Dr. Lutz Nasdala

Acknowledgments

First of all, I want to thank Lutz Nasdala, who gave me the opportunity to work on this thesis and invested a lot of time supervising it. I also have to thank Andreas Artač, Christoph Lenz and Manuela Zeug for having a helpful answer to any question I might have had and Simon Steger for providing all results of his bachelor thesis.

I also want to thank everybody who made samples available for investigation, i.e. Elias Chatzitheodoridis, Andrew Cross, Larissa Dobrzhinetskaya, Jakub Grulya, Andrey Korsakov, Hans-Joachim Massonne, Igor V. Pekov, Benjamin Rondeau, Maria D. Ruiz-Cruz, Andy H. Shen, Bhuwadol Wanthanachaisaeng and Petr Zaunstöck. Special thanks go to Andreas Wagner, who not only provided samples, but also prepared all samples for investigation.

Declaration

I hereby declare that this thesis contains no material, which has been submitted or accepted for an award of any other degree or diploma in any university or institution. To the best of my knowledge and belief this thesis contains no material previously published by any other person except where acknowledgment has been made.

Vienna, 2015

Claudia Reissner

Abstract

This thesis addresses the question whether or not it is possible to distinguish naturally formed UHP (ultrahigh pressure) diamond and diamond particles originating from abrasives based on their Raman spectra. Samples investigated comprised (i) seventeen diamond abrasives (characterised by a range of grain sizes, and originating from 6 different manufacturers), and (ii) five natural microdiamond samples coming from four UHP locations (Ceuta, Spain; Kokchetav Massif, Kazakhstan; Saidenbach reservoir, Germany; and Rhodope Mountains, Greece). It was found that for both types of sample, Raman parameters (i.e. Raman shift and FWHM, full width at half maximum), may deviate from that of the ideal diamond Raman spectrum. Diamond abrasives are characterised by moderate to appreciable band broadening (FWHMs up to 12.6 cm^{-1}) that may, or may not, be accompanied by band down-shift (Raman shifts down to 1316 cm^{-1}). For the assumed UHP sample from Ceuta, no unambiguous UHP microdiamond was found. The UHP-diamond samples from Kokchetav, Saidenbach, and the Rhodopes, showed moderate FWHM increase (FWHMs up to $\sim 6.5\text{ cm}^{-1}$) accompanied by either moderate down- or even very minor up-shift (Raman shifts in the range $1329.6\text{--}1332.7\text{ cm}^{-1}$). Spectral trends of abrasives and UHP microdiamond hence overlap partially. This excludes reliable assignment of diamond found in geological samples from the Raman spectra alone. Criteria to distinguish genuine UHP microdiamond and diamond artefacts originating from sample preparation are discussed critically.

Deutsche Zusammenfassung

Diese Masterarbeit befasst sich mit der Frage, ob es möglich ist, natürlich entstandene UHP (*Ultra-High Pressure* = Ultrahochdruck) Diamanten und Diamantpartikel aus Schleifmittel auf der Grundlage ihrer Raman-Spektren zu unterscheiden. Die untersuchten Proben umfassten (i) 17 Diamant-basierte Abrasiva (unterschieden durch ihren Korngrößenbereich und von sechs verschiedenen Herstellern erzeugt), und (ii) fünf natürlichen Mikrodiamantproben aus vier UHP Gebieten (Ceuta, Spanien; Kokchetav Massif, Kasachstan; Saidenbach Reservoir, Deutschland und Rhodopen, Griechenland). Es wurde festgestellt, dass für beide Probenarten die Raman-Parameter, d.h. Ramanverschiebung und FWHM (*Full Width at Half band Maximum* = Banden-Halbwertsbreite) von denjenigen der idealen Raman-Spektren von Diamant abweichen können. Diamant-Schleifmittel werden von mittlerer bis starker Bandenverbreiterung gekennzeichnet (Halbwertsbreiten von bis zu $12,6 \text{ cm}^{-1}$), die mit einer Verschiebung der Bandenposition zu niedrigerem Raman shift einhergehen kann (Raman shift bis auf 1316 cm^{-1}). Für die angebliche UHP Probe von Ceuta, wurde kein eindeutiger UHP Mikrodiamant gefunden. Die UHP-Diamant-Proben aus Kokchetav, Saidenbach und den Rhodopen, zeigten eine leichte Erhöhung der FWHM (Halbwertsbreiten bis zu $\sim 6.5 \text{ cm}^{-1}$), begleitet von einer leichten Rot- oder sogar sehr geringer Blau-Verschiebung (Raman-Verschiebungen im Bereich von $1329,6$ bis $1332,7 \text{ cm}^{-1}$). Spektrale Trends von Schleifmitteln und UHP Mikrodiamanten überlappen damit teilweise. Dies schließt sichere Zuordnung von Diamant, welcher in geologischen Proben gefunden wurde, allein auf Grund der Raman-Spektren aus. Kriterien zur Unterscheidung zwischen echten UHP Mikrodiamanten und Diamant-Artefakten aus der Probenvorbereitung werden kritisch diskutiert.

Table of Content

Acknowledgments	3
Declaration	5
Abstract	7
Deutsche Zusammenfassung	9
Table of Content.....	11
1. Introduction	13
2. Raman Spectroscopy.....	16
2.1 The Raman Effect.....	16
2.2 Analytical Settings.....	17
2.3 FWHM Correction.....	18
3. Diamond.....	19
3.1 Generalities.....	19
3.2 Raman Spectra.....	21
4. Samples	23
4.1 Abrasives.....	23
4.2 Natural UHP-Microdiamond samples.....	30
5. Results and Discussion	34
5.1 Diamond-based abrasives	35
5.2 Natural UHP microdiamond	37
6. Appendices.....	40
Appendix I: Data table	40
Appendix II: Additional figures	43
Appendix III: List of Figures.....	46
Appendix IV: List of Tables.....	48
Appendix V: References.....	48
Appendix VI: Curriculum vitae	51

1. Introduction

Given that diamond can only be formed at temperatures above 900°C and pressures of 4 GPa and higher, this mineral is often considered as an index mineral for ultra-high pressure (UHP) metamorphism (Smith 1984). The reliability of the mere presence of diamond as UHP indicator is however hampered by the fact that geological samples may, as an analytical artefact, contain diamond particles that originate from the sampling and preparation process. Due to its exceptional hardness (Vickers hardness $\sim 10.000 \text{ kp/mm}^2$; hardness 10 on the Mohs scale), diamond is a common abrasive material. As relevant for geological samples, this includes diamond tools (e.g. core drill, saw) and preparation abrasives (e.g. grinding and polishing materials). Such diamond particles may be uptaken by rock or mineral samples, for instance being captured in fractures or pores.

Diamond artefacts originating from tools or abrasives may be interpreted wrongly as naturally formed UHP diamond; this may then have far-reaching consequences. To give an example, in an article in the top-ranked journal Nature Menneken et al. (2007) claimed to

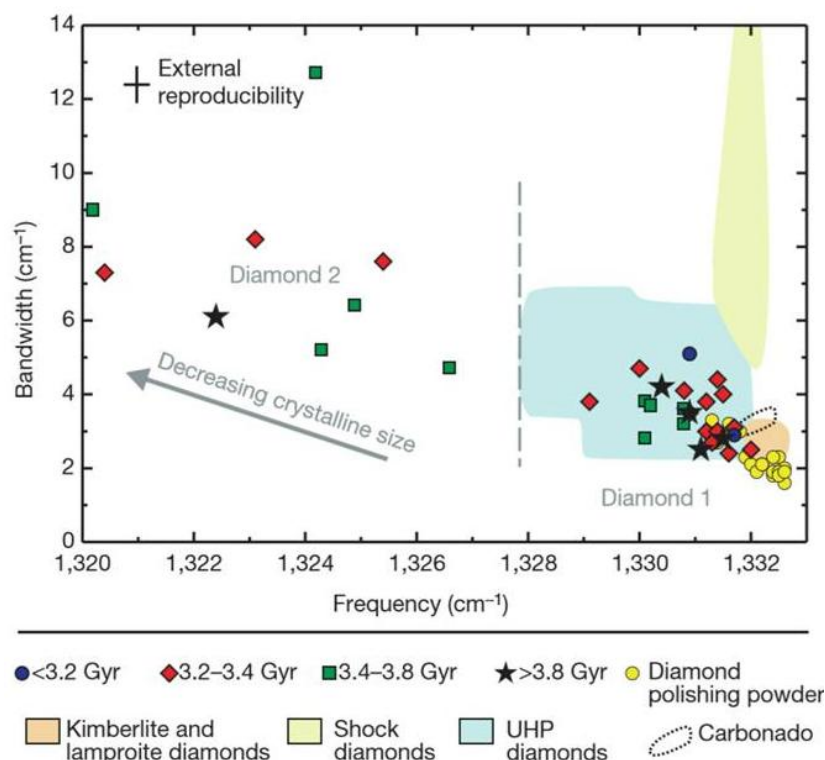


Fig.1 Comparison of Raman shift and bandwidth of diamond samples (image from Menneken et al. 2007)

have found UHP microdiamond in Hadean zircon from a metaconglomerate from the Jack Hills, Western Australia. These authors concluded that as early as 4,300 myr ago, the Earth's crust must have been thick enough (i.e. well more than 140 km) to achieve UHP conditions. If confirmed to be true, this finding would have added to our knowledge on the early history of our planet.

Attempting to address the problem described above, Menneken et al. (2007) considered the possibility their samples might be contaminated by diamond-abrasive material. They therefore compared spectroscopic parameters of the diamond in their thin sections with parameters of the diamond-based polishing powder used to prepare those sections. Results are shown in Fig.1, which is a plot of Raman shift against full width at half maximum (FWHM) of the main Raman band of diamond. Data pairs obtained from the polishing powder (Raman shift $\sim 1332 \text{ cm}^{-1}$; $\text{FWHM} \leq 4 \text{ cm}^{-1}$) plot fairly close to the Raman parameters of ideal diamond (Solin & Ramdas 1970; cf. discussion in chapter 3.2 below). The diamond detected in the Jack Hills sample, in contrast, showed strong decreases of the Raman shift accompanied by significant increases of the FWHM. The obvious mismatch of the two sets of Raman data led Menneken et al. (2007) to the conclusion that the diamond in their sample cannot be a result of contamination but must be genuine UHP microdiamond.

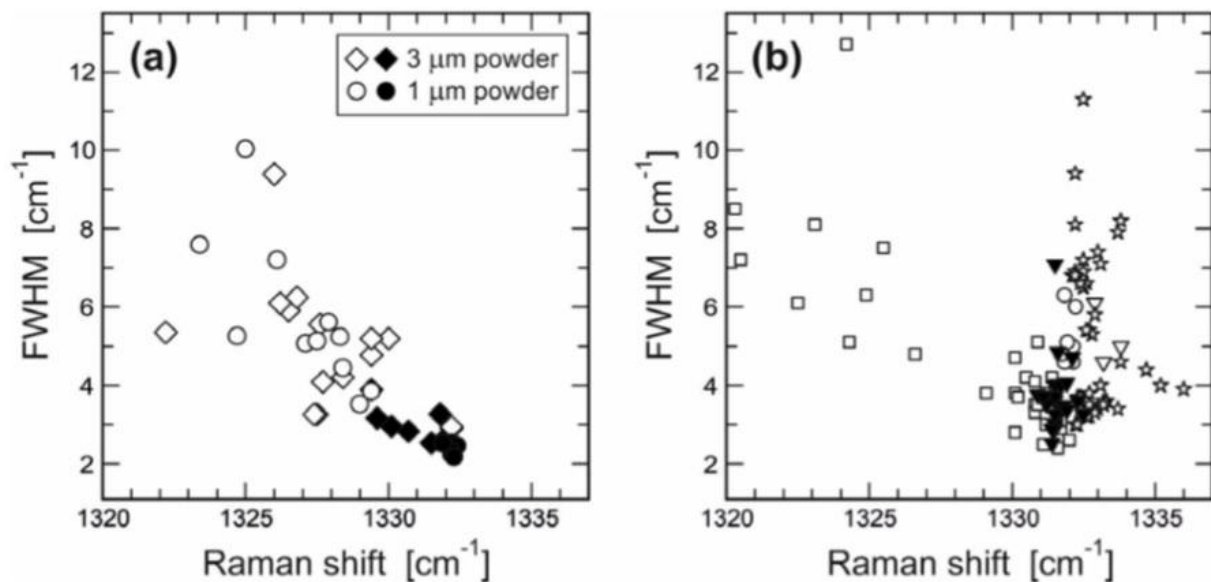


Fig.2 Plots of Raman spectral parameters of the main diamond band. (a) Two diamond-based MRB abrasives (Resin bond diamond powder, Mant USA, Inc.; open symbols = fresh powders; full symbols = used powders). (b) UHP microdiamond (full symbols = present work; open symbols = data from Menneken et al. 2007 and Perraki et al. 2009; ▽ = Saidenbach, Erzgebirge, Germany; □ = Jack Hills, Western Australia; ○ = Rhodopes, Greece; ☆ = Kokchetav, Northern Kazakhstan). (from Steger et al. 2013)

Recently Steger et al. (2013) conducted a study addressing potential differences between Raman spectra of fresh diamond-based abrasives and their used analogues. These authors found that Raman parameters of fresh and used abrasives may differ appreciably (Fig.2Fig.2a). For the example of Resin bond diamond powder, Mant USA, Inc., the considerable decrease of initial Raman-band downshift and broadening were observed after use of the abrasive. This is explained by the particular synthesis resulting in initial stress of the diamond particles, which then results in easy breaking and hence “self-sharpening” accompanied by the release of stress.

In a comprehensive transmission electron microscopy study, Dobrzhinetskaya et al. (2014) have examined the very same diamond samples that were investigated and described earlier by Menneken et al. (2007). Dobrzhinetskaya et al. (2014) found diamond particles only in surficial pockets, along with gold and epoxy, but never included in the bulk zircon. They therefore concluded that the diamond detected by Menneken et al. (2007) was due to sample contamination originating from diamond-based polishing powder used in the sample-preparation process. This example verifies again that the distinction of naturally formed and occurring microdiamond and diamond-based abrasive material therefore is a very important issue. The problem has been addressed already by various scientists (e.g. Perraki et al. 2009).

The present MSc thesis aims at comparing results of Raman-spectroscopic measurements on natural UHP-diamond samples with analogous results obtained from diamond abrasives. The main question was, is it possible to distinguish reliably UHP-diamond and diamond abrasives based on Raman-spectroscopic data?

2. Raman Spectroscopy

2.1 The Raman Effect

The Raman Effect describes inelastic scattering of light on atoms or molecules. During this process, a small part of the energy of the light will be transferred to the atoms/molecules as vibration energy (in the very uncommon case of an anti-Stokes scattering, see below, the energy will be added to the light). Thus the emitted light will have a different energy than the exciting light.

The vibration energy can only occur at discrete levels with rather low energy. Since Raman spectroscopy usually uses excitation wavelength in the visible light spectrum (including near infrared, NIR, and ultraviolet, UV), the excitation energy is higher than the energy difference of two vibration levels. If the excitation wavelength is exactly the same energy as the difference between two levels, infrared absorption would occur (Fig.3.1). If the light is elastically scattered at the atoms, the energy of the light does not change, which is called Rayleigh scattering (Fig.3.2). If the light is scattered inelastically, the scattering might be of Stokes type or anti-Stokes type. In the case of Stokes-type scattering, the vibration energy is excited to a higher energy level through excitation by the light. Therefore, the emitted light's energy would be equivalent to the excitation energy minus the energy difference of the two

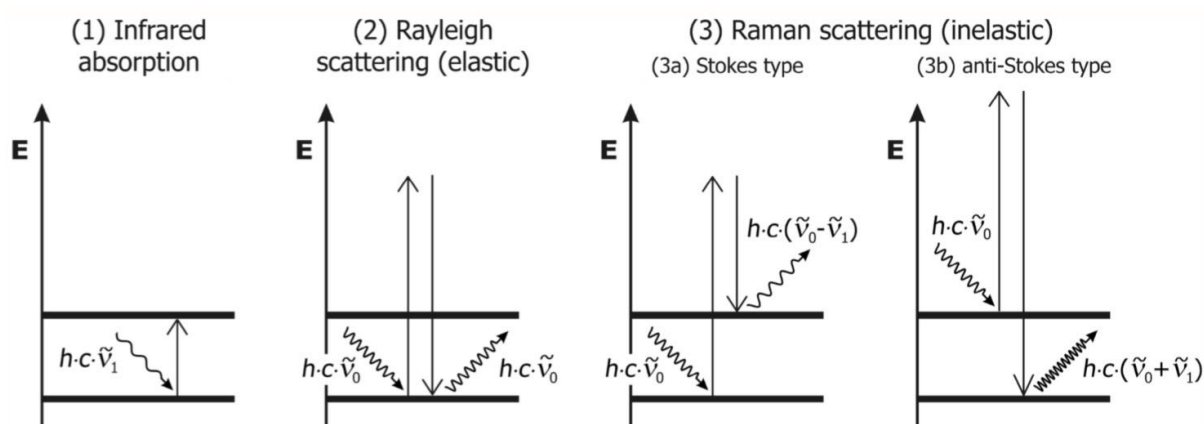


Fig.3 Elucidation of the light-molecule interaction using a simplified energy level diagram. (1) Infrared absorption. (2) Rayleigh scattering (3) Raman scattering with (3a) Stokes type and (3b) anti-Stokes type (Nasdale et al. 2004).

vibration levels (Fig.3.3a). If the vibration energy is already in an excited state, the anti-Stokes scattering lowers it to a lower level which leads to a higher energy of the emitting light than the excitation energy (the difference being again the difference between the two vibration levels) (Fig.3.3b).

Since Raman spectroscopy measures differences of energy levels it can be excited with light of any discrete energy. Due to the decreased probability of the Raman effect at lower energies, and the technical difficulty of detection at higher energies, visible light (including NIR and UV) is used in most cases. The spectra of the Stokes type and the anti-Stokes type are symmetrical in respect to the Rayleigh line, though the probability of a Stokes type scattering is much less than an anti-Stokes type scattering. This leads to higher intensities in the Stokes spectrum, wherefore mostly the Stokes spectrum is investigated. For more detailed explanations see for example Nasdala et al. 2004.

2.2 Analytical Settings

All measurements were performed on a Horiba Jobin Yvon Lab Ram HR Evolution spectrometer equipped with a Olympus BX41 microscope and a CCD detector. A 50x long distance lens has been used. The spectrometer allows one to switch between a 600 gr/mm and a 1800 gr/mm grid, all measurements shown in this work have been executed using the 1800 gr/mm grid. The excitation wavelength has mostly been 633 nm, although in some cases, because of a strong luminescence of the samples in this range, a 532 nm laser has been used. The confocal slit has been at a maximum of 500 μm . The band position and full width at half maximum (FWHM) were determined using the Peakfit® software. Fitting was done after appropriate background correction. As the obtained bands consist of an overlap of the predominantly Lorentzian Raman band and the Gaussian shaped apparatus function, combined Gaussian-Lorentzian band shapes were assumed in the fit procedure.

2.3 FWHM Correction

By means of mechanical and technical limitations, the bands in the spectra may experience a broadening, which has been corrected by using the formula by Dijkman & van der Maas (1976; see also Tanabe & Hiraishi 1980 and Irmer 1985):

$$b = b_s * \sqrt{1 - 2 * \left(\frac{s}{b_s}\right)^2}$$

with b = *real FWHM*, b_s = *measured FWHM*, and s = *apparatus function of the Raman spectrometer*. Here, the system's apparatus function s was assumed as 0.8 cm^{-1} .

3. Diamond

3.1 Generalities

Diamond is an element mineral. It consists of native carbon that crystallises in space group $Fd3m$. This material shows perfect {111} cleavage. Diamond has the highest thermal conductivity and the highest hardness of any known substance (Anthony et al. 1990).

Boron and nitrogen traces cause structural defects in diamond crystals, which are detected mostly via infrared absorption spectroscopy. According to the existence of such defects diamond samples are divided into different Types (Breeding and Shigley 2009). Where Types Ia and Ib show a large number of nitrogen based defects, Types IIa and IIb on the other hand show little to no defects caused by nitrogen.

Diamond can be formed in different ways. The biggest crystals come from high depths with pressures of at least 4 GPa and temperatures starting at 900°C (Smith 1984) as an early pro-

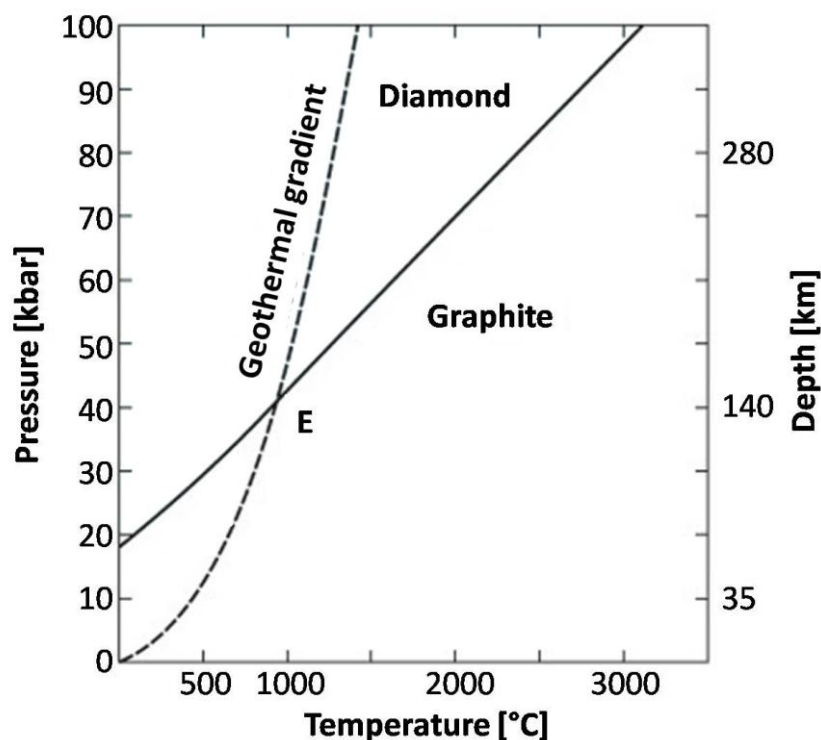


Fig.4 Phase diagram for carbon, visualising the stability fields of graphite (α -C) and diamond (β -C). Point E (900°C, ~40 kbar) marks the minimum pressure and temperature conditions needed for the transformation of graphite to diamond. They correspond to a theoretical depth of about 140 km below the Earth's surface (from Ernst 1976; modified).

duct in ultrabasic magma and are transported in pipes, or similar, to the surface. Due to the fast transport to the surface, the diamond crystal is not reconverted to graphite. In contrast, metamorphic rocks are mostly exhumated rather slow. The first microdiamond in metamorphic rocks was described by Sobolev & Shatsky 1990. This diamond can occur metastable at the Earth's surface due to the high activation energy needed for the reversion to graphite. This reversion would also lead to a high increase in volume, since the structural density of graphite is much less than the density of diamond. Therefore, microdiamond embedded in a rigid host mineral (zircon, garnet, etc.) might endure a slow exhumation, since the persistency of the host mineral counteracts the volume increase. If the diamond exceeds a certain critical size (for the Saldenbach locality about 30 μm), the stress caused by the diamond to the surrounding host mineral would lead it to break and the diamond would then transform to graphite.

Magmatic diamond often contains inclusions of mantle material. It is therefore an important mineral in the Earth sciences, especially in the field of mantle petrology. Detailed investigation of such inclusions may provide valuable information on the diamond's origin (Koivula 2000; Nasdala et al. 2003). For example, Pearson et al. (2014) discovered terrestrial ringwoodite inclusions in a diamond from Juína, Brazil. Since ringwoodite is only formed in the Earth's lower transition zone (i.e. at about 520–660 km depth below the Earth's surface), this ringwoodite inclusion is an excellent indicator of the depth the host diamond was formed.

The valence-conduction band gap of diamond is 5.45 eV (Sauer 1999), which makes this mineral a perfect isolator crystal. However, diamond may show semiconductor properties owing to the incorporation of trace elements (e.g. boron, sulphur) that create introduced electronic levels within the forbidden band gap. Diamond is therefore used commonly in electronic systems (Sauer 1999). Other industrial applications of this mineral include, among others, polishing and cutting materials, advanced tools such as medical scalpels, thermal management, resistant coatings – here however especially CVD (chemical vapour deposition) grown diamond films – and optics. The use of diamond as gemstone includes its use as international currency (especially drug trade).

3.2 Raman Spectra

Ideal diamond yields a single, narrow band in its Raman spectrum with a Raman shift of 1332.5 cm^{-1} ($\pm 0.5 \text{ cm}^{-1}$) and a FWHM of about 1.65 cm^{-1} ($\pm 0.02 \text{ cm}^{-1}$) (Solin & Ramdas 1970). This band is caused by three different vibration modes. Due to the high symmetry of diamond those modes are at an equivalent energy which leads to a single, triply degenerate band.

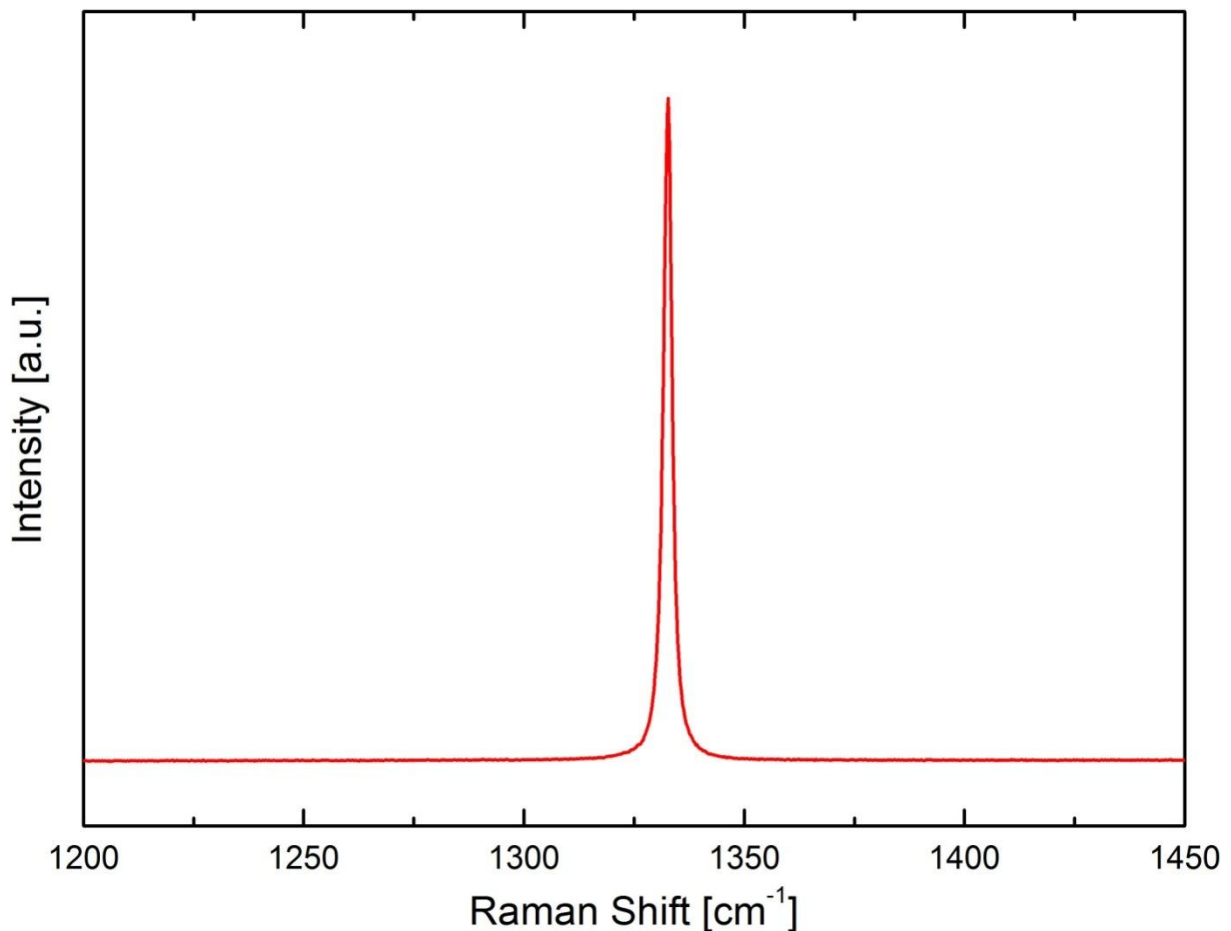


Fig.5 Raman spectrum of an unstressed diamond. Raman shift: 1332.6 cm^{-1} ; FWHM: 2.3 cm^{-1} .

Both Raman shift and FWHM may vary. Solin & Ramdas (1970) reported increased FWHMs at higher temperatures, accompanied by decreased Raman shifts. Similar variations of band parameters may also be caused by radiation damage (Jamieson et al. 1995) or enhanced ^{13}C concentration (Hass & Tamor 1992). Stress also has a strong influence on the Raman spectra of diamond. Tensile stress results in lowered Raman-shift values whereas

compressive stress results in increased Raman shifts; which are in both cases often accompanied by notable band broadening and increasing deviation from the ideal symmetric band shape (Knight & White 1989, Sharma et al. 1985).

This stress-induced variation of the Raman shift is caused by a change of the bonding lengths, which leads to altered vibration energy levels. Tensile stresses, where the crystal is "inflated", cause an elongation of the bonds, resulting in a decreased Raman shift. Compressive stresses, which "shrink" the crystal, causes a shortening of the bonds, resulting in an increased Raman stress. Both cases cause an increased FWHM. Not all the bonds in the crystal are elongated/shortened equally, the increased FWHM reflects the statistical variance of the Raman shift in the crystal.

4. Samples

4.1 Abrasives

The main interest considered for the choice of abrasives, was to get a wide range of samples from different sources and origins. Seven laboratories were contacted for samples of diamond-based abrasives, and asked for as much information as possible on manufacturer and grain size. Six labs provided polishing pastes and one provided polishing powder. Except for the sample from Wuhan, the grain sizes of all abrasive materials were stated. The manufacturer on the other hand was not always known.

Table 1 Providers of diamond-based abrasives.

Name	Institution	City	Country
Jakub Grulya, Petr Zaunstöck	Department of Geological Sciences, Masaryk University	Brno	Czech Republic
Andrew Cross	Geochronology Laboratory, Geoscience Australia	Canberra	Australia
Bhuwadol Wanthanachaisaeng	Faculty of Gems, Burapha University	Chanthaburi	Thailand
Igor V. Pekov	Faculty of Geoscience, Lomonosov Moscow State University	Moscow	Russia
Benjamin Rondeau	Laboratoire de Planétologie et Géodynamique, Université de Nantes	Nantes	France
Andreas Wagner	Institute for Mineralogy and Crystallography, University of Vienna	Vienna	Austria
Andy H. Shen	Institute of Gem and Jewellery Studies, China University of Geosciences	Wuhan	China

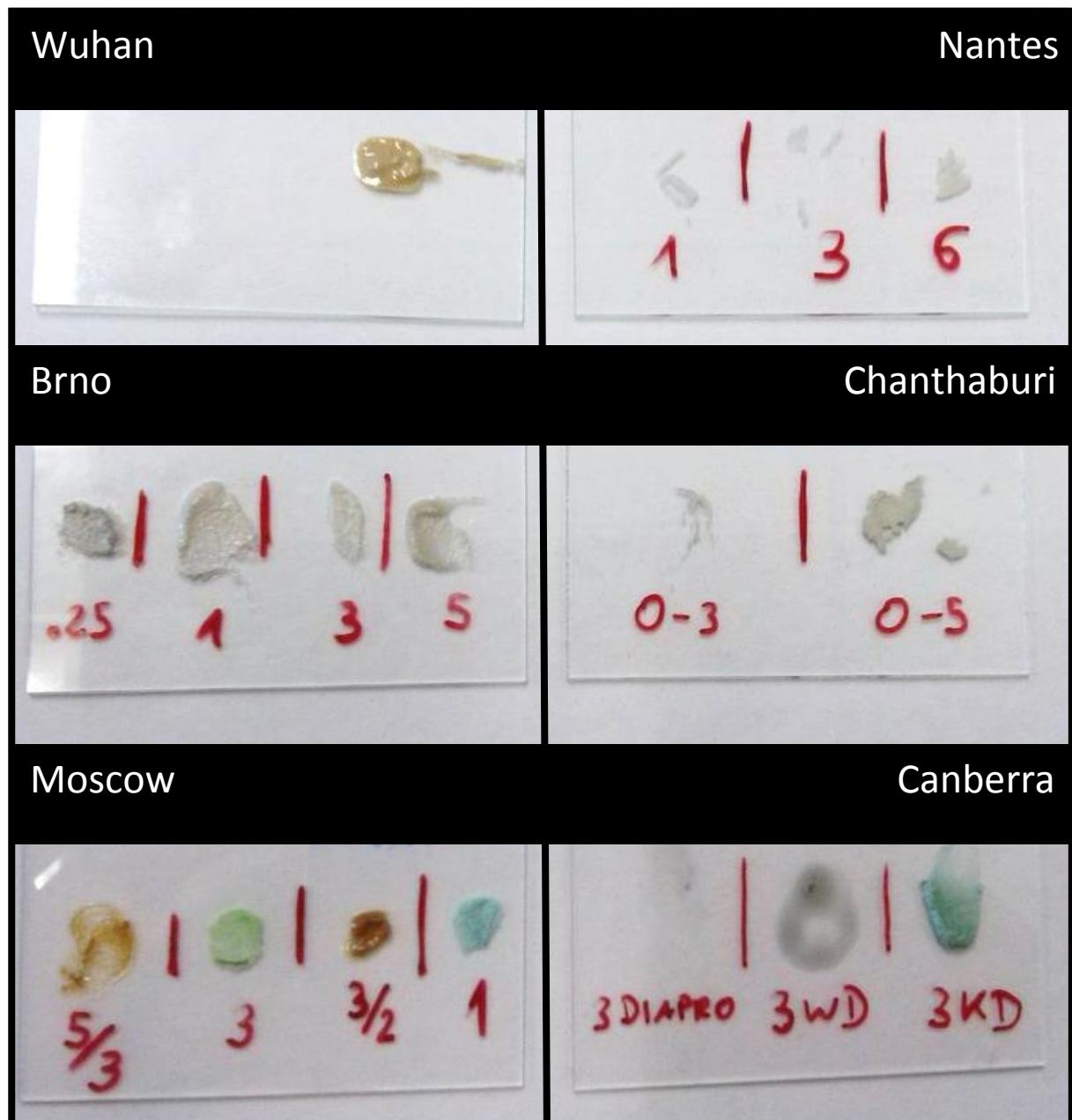


Fig.6 Polishing paste samples on object slides. The city names show the location of the laboratories that sent the samples (note that these locations do not correspond to the manufacturing origin). The numbers show the grain size in μm , respectively the product name (Canberra).

Brno

The polishing pastes from Brno, Czech Republic, with grain sizes of 0.21, 1, 3, and 5 μm , were manufactured by the company Struers. This is a globally delivering company with its head office in Willich, Germany.

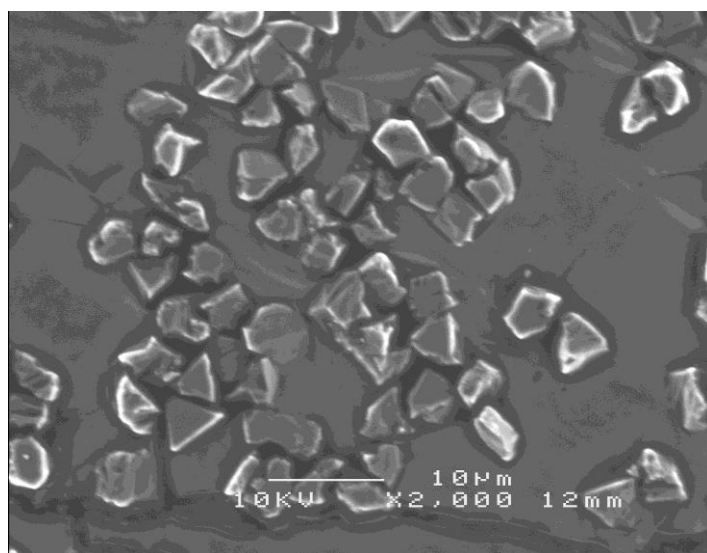


Fig.7 Back scattered electron microscopy (BSE) image of the Brno abrasive (grain size: 5 μm).

Canberra

From Canberra 3 different samples, all with a grain size of 3 μm , have been sent. Due to its strong luminescence signal, it was not possible to measure Raman spectra with the available lasers.

Chanthaburi

Two polishing pastes have been provided from Chanthaburi, Thailand, with a grain size range of 03 respectively 05 μm . Those have been purchased from a local dealer who sells his products in Thailand exclusively. The diamond particles are most likely originated from China, though it is unknown, whether they are of natural origin or synthesised crystals.

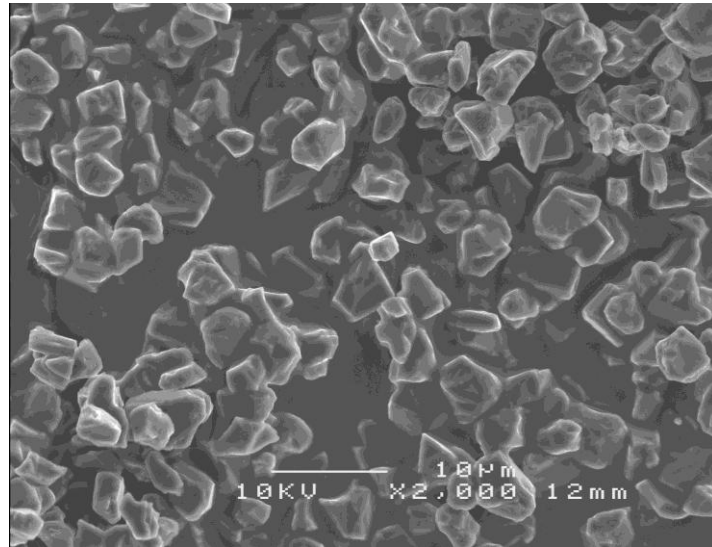


Fig.8 BSE image of the Chanthaburi abrasive (grain size: 0–5 μm)

Moscow

From Moscow, Russia, two different types of samples have been sent. With a grain size of 1 respectively 3 μm , a product of the US-American company Buehler and with a grain size range of 23 respectively 35 μm , polishing pastes sold by a local Russian firm during the 1980s which does not exist anymore.

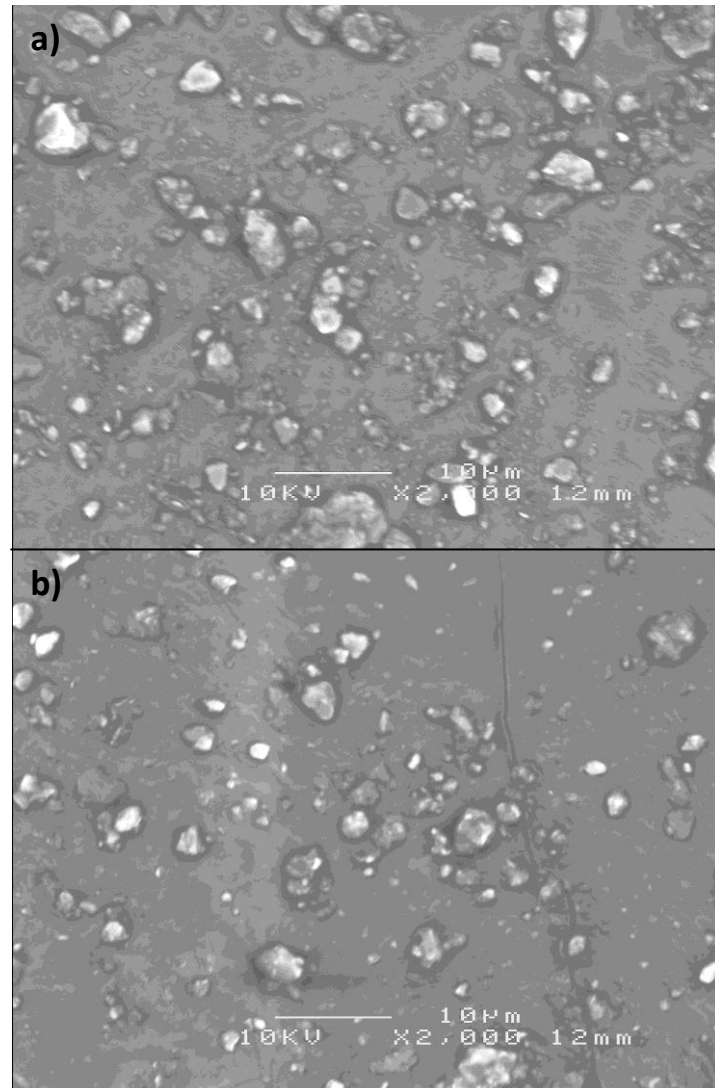


Fig.9 BSE image of the Moscow abrasives a) from the company Buehler (grain size: 3 μm) b) from a local Russian manufacturer (grain size: 2–3 μm)

Nantes

The polishing pastes provided from Nantes with a grain size of 1, 3 and 6 μm , were manufactured by the French company Escil. They deliver mainly in France with their head office located in Chassieu.

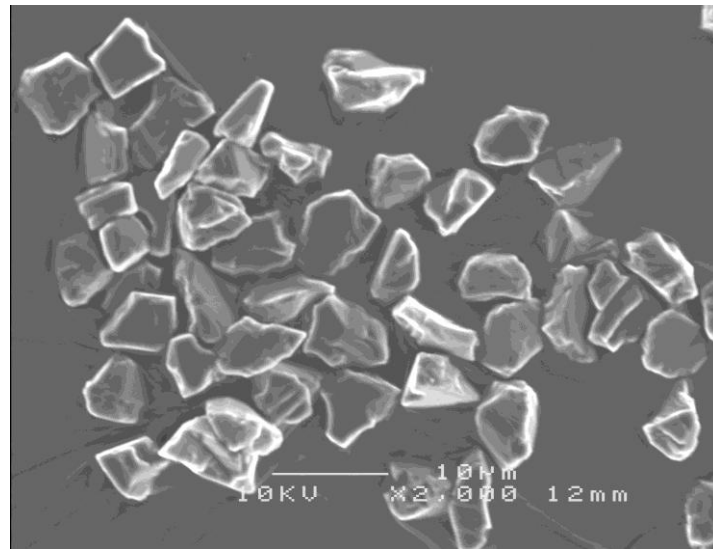


Fig.10 BSE image of the Nantes abrasive (grain size: 6 μm).

Vienna

Polishing powders with a grain size of 0.25, 1 and 3 μm from the in-house workshop of the Institute of Mineralogy, University of Vienna, were examined. They were products of the US-American company Mant USA, Inc.

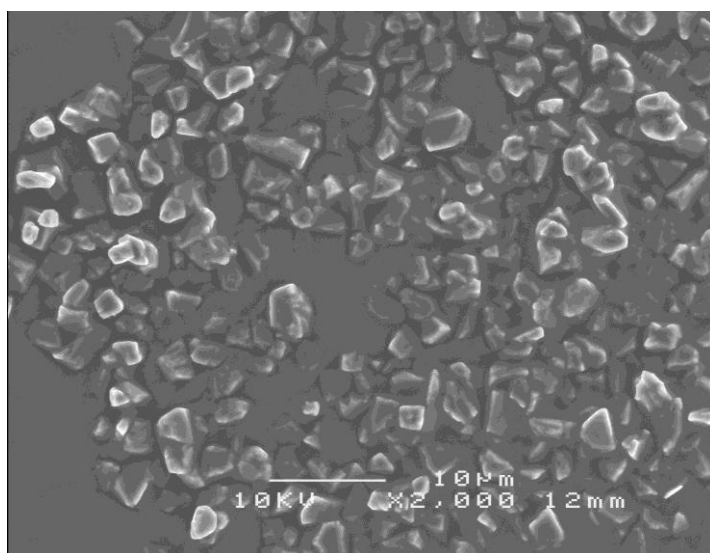


Fig.11 BSE image of the abrasive from Vienna (grain size: 3 μm).

Wuhan

Unfortunately, no information could be provided about the polishing paste from Wuhan, China. From microscopic studies a maximum grain size of 2 μm could be determined. More precise studies have not been possible during this work.

4.2 Natural UHP-Microdiamond samples

Seven different UHP locations have been selected to be investigated (Ceuta, Spain; České středohoří Mountains; Czech Republic; Kokchetav Massif, Kazakhstan; Qinling, central China; Rhodope Mountains, Greece; Saidenbach reservoir, Germany; Tromsø Nappe, Norway). Unfortunately only samples from four of those locations could be acquired (i.e. Ceuta, Kokchetav Massif, Saidenbach reservoir, Rhodope Mountains).

Table 2 Providers of UHP microdiamond samples.

Name	Institution	Origin of sample
Maria Dolores Ruiz Cruz	Departamento de Químicalnorgánica, Cristalografía y Mineralogía Facultad de Ciencias, Universidad de Málaga, Spain	Ceuta, Spain
Andrey Korsakov	Institute of Geology and Mineralogy Siberian Branch, Russian Academy of Sciences, Novosibirsk, Russia	Kokchetav Massif, Kazakhstan <i>In-situ diamond</i>
Larissa Dobrzhinetskaya	Departement of Earth Sciences, University of California, Riverside United States of America	Kokchetav Massif, Kazakhstan <i>Excavated diamond</i>
Hans-Joachim Massonne	Institut für Mineralogie und Kristallchemie, Universität Stuttgart, Germany.	Saidenbach reservoir, Germany
Elias Chatzitheodoridis	Department of Geological Sciences, National Technical University of Athens, Greece	Rhodope Mountains, Greece

Ceuta

Ceuta is located north of Morocco at the Mediterranean Sea. The investigated sample is of granulites from the Betic-Rif Cordillera, a part of the alpine orogeny. The Cordillera is split into an internal and an external zone, where the external zone consists of sediments from the Triassic to Miocene. The internal zone consists of metamorphic rocks from the Palaeozoic to the Tertiary. (Ruiz-Cruz & Sanz de Galdeano 2012)

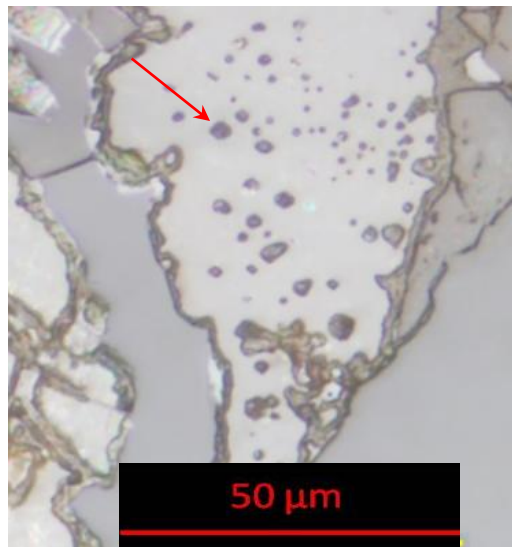


Fig.12 Reflected-light image of an assumed microdiamond (marked with arrow) in garnet, from Ceuta, Spain.

Kokchetav Massif

The Kokchetav Massif, located on a suture zone, is part of the Central Asian Orogenic Belt (CAOB) (Schertl & Sobolev 2012). Diamond particles were found in the ultra-high pressure belt, consisting of precambrian protoliths (Kaneko et al. 2000).

Two different samples have been examined during this work. First, excavated diamond crystals, second, rock-sections with diamond still inside and fully embedded in the host mineral garnet.

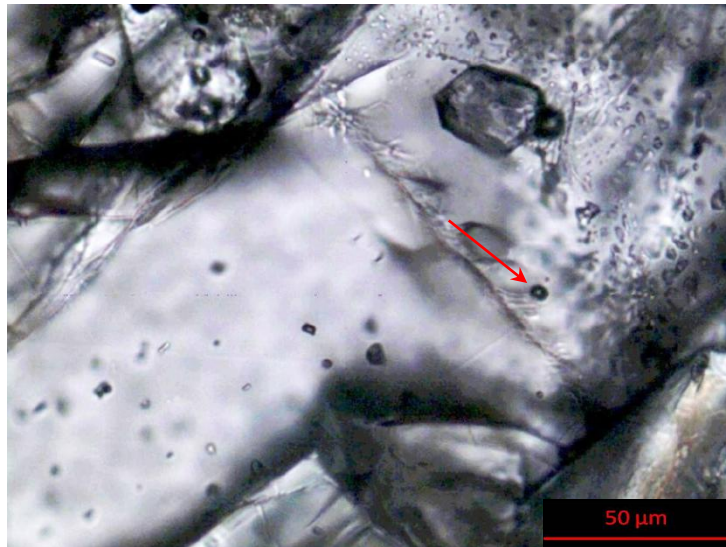


Fig.13 Plane-polarised transmitted-light microphotograph of a garnet from the Kokchetav Massif. The microdiamond is marked with an arrow.

Rhodope Mountains

The Rhodope Mountains are located at the border between Greece and Bulgaria. The investigated sample is from the Nestos fault line in the Greek part of the mountains. This zone includes a several hundred meter thick layer of fine grained biotite gneisses, amphibolites, granitic gneisses and garnet-mica schists (Schmidt et al. 2010). Here, too, the diamond has been completely embedded in the host mineral (garnet).

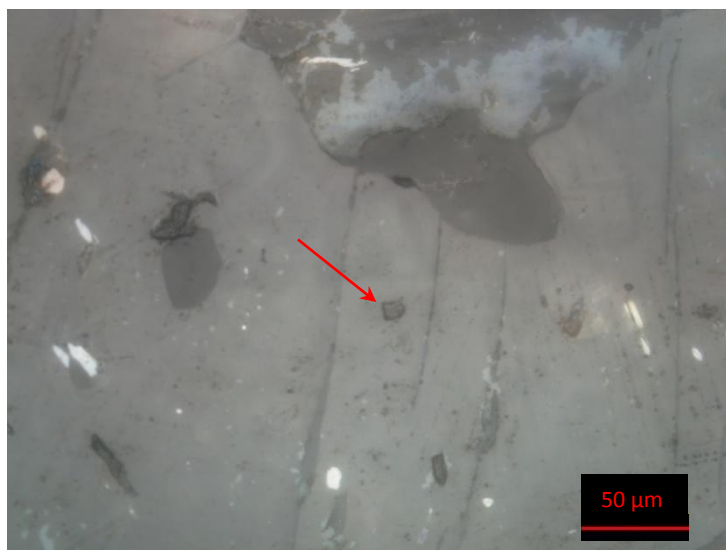


Fig.14 Reflected-light image of a thin section from the Rhodope Mountains, Greece. A small diamond is marked with an arrow.

Saidenbach reservoir

The Saidenbach reservoir, Germany, is located in the Saxonian Erzgebirge, a late-palaeozoic part of the Bohemian Massif (Massonne 2003). Microdiamond grains have been found in gneisses from this region (Nasdala & Massonne 2000), which have been available for measurements. Like in the sections from the Kokchetav Massif and the Rhodope Mountains, the diamond particles were completely beneath the surface and embedded in their host mineral (here: zircon).



Fig.15 Plane-polarised transmitted-light image of diamond inclusions in a zircon grain from the Saidenbach reservoir, Germany. Note the focus is well beneath the polished sample surface.

5. Results and Discussion

The Raman spectra of diamond-based abrasives showed extensive variations whereas the Raman spectra of natural microdiamond were less variable. Results are listed in Tables 3 and 4 (Appendix I), and plots of Raman-band parameters (i.e. FWHM versus Raman shift) are

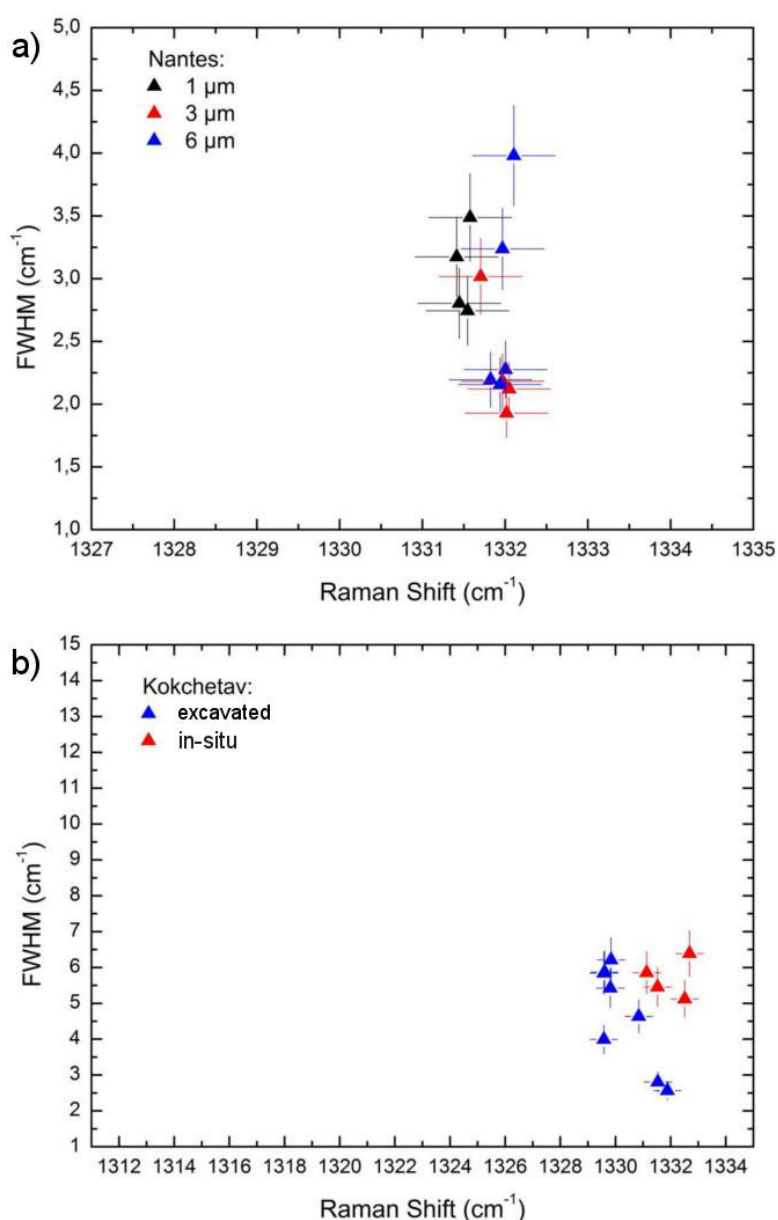


Fig.16a) Plot of FWHM against Raman shift of the main diamond Raman band, for abrasives of different grain size from Nantes. b) Analogous plot for two samples of natural UHP diamond from the Kokchetav Massif. All measurements were taken with He-Ne 632.8 nm excitation.

presented in Figs. 16–18. For more complete visualisation of the results, additional figures (Figs. 19–23) are presented in Appendix II.

5.1 Diamond-based abrasives

Six out of the seven laboratories have provided abrasives of different grain size. It was therefore possible to check whether or not the grain size has any effect on the spectral parameters of the main Raman band of diamond. Whereas spectral parameters differ among abrasives from different manufacturers, no significant effect of the grain size was found, that is, abrasives of different grain size from one and the same manufacturer yielded the same parameters within errors. As an example the Raman parameters of differently sized abrasive samples from Nantes are shown in Fig.16a. Equivalent figures for all other samples are provided in Appendix II.

As shown in Fig. 16a the grain size causes little to no alteration of the Raman shift and FWHM. Recently, Steger et al. (2013) has measured a range of diamond-based abrasives, with the aim to study possible effects of the abrasion procedure on spectra. He found that fresh (i.e. unused) abrasives may show strongly decreased Raman shifts and increased FWHMs, when compared to the theoretical spectral parameters of diamond (compare Solin & Ramdas 1970). At a first glance, his results seem to be supported by the results of the present MSc work (Fig.17a). However, downshifts of band positions and increases of FWHMs is not a feature typical of all abrasive. As it can be seen in Figs.17b–c, such deviations from perfect diamond are only observed from the samples from Vienna and Chanthaburi, which are characterised by Raman shifts in the range $1316\text{--}1332\text{ cm}^{-1}$ and FWHMs in the range $2.6\text{--}12.6\text{ cm}^{-1}$. All other abrasives show comparatively little variation in their Raman-shift values ($1331.4\text{--}1332.2\text{ cm}^{-1}$) and FWHMs ($1.8\text{--}4.0\text{ cm}^{-1}$). The observed variations in Raman parameters of the abrasives from Vienna and Chanthaburi are most likely caused by tensile stress. At least for the Vienna samples it is known that their manufacturer (Mant USA, Inc.) produces synthetic diamond that is stressed intentionally. This treatment eases the breaking of the crystals during the polishing process, which results in the formation of new, sharp edges("The specific friability and semi-blocky shape offers consistent performance by ensuring a constant supply of new cutting surfaces." Mant USA, Inc.2014).

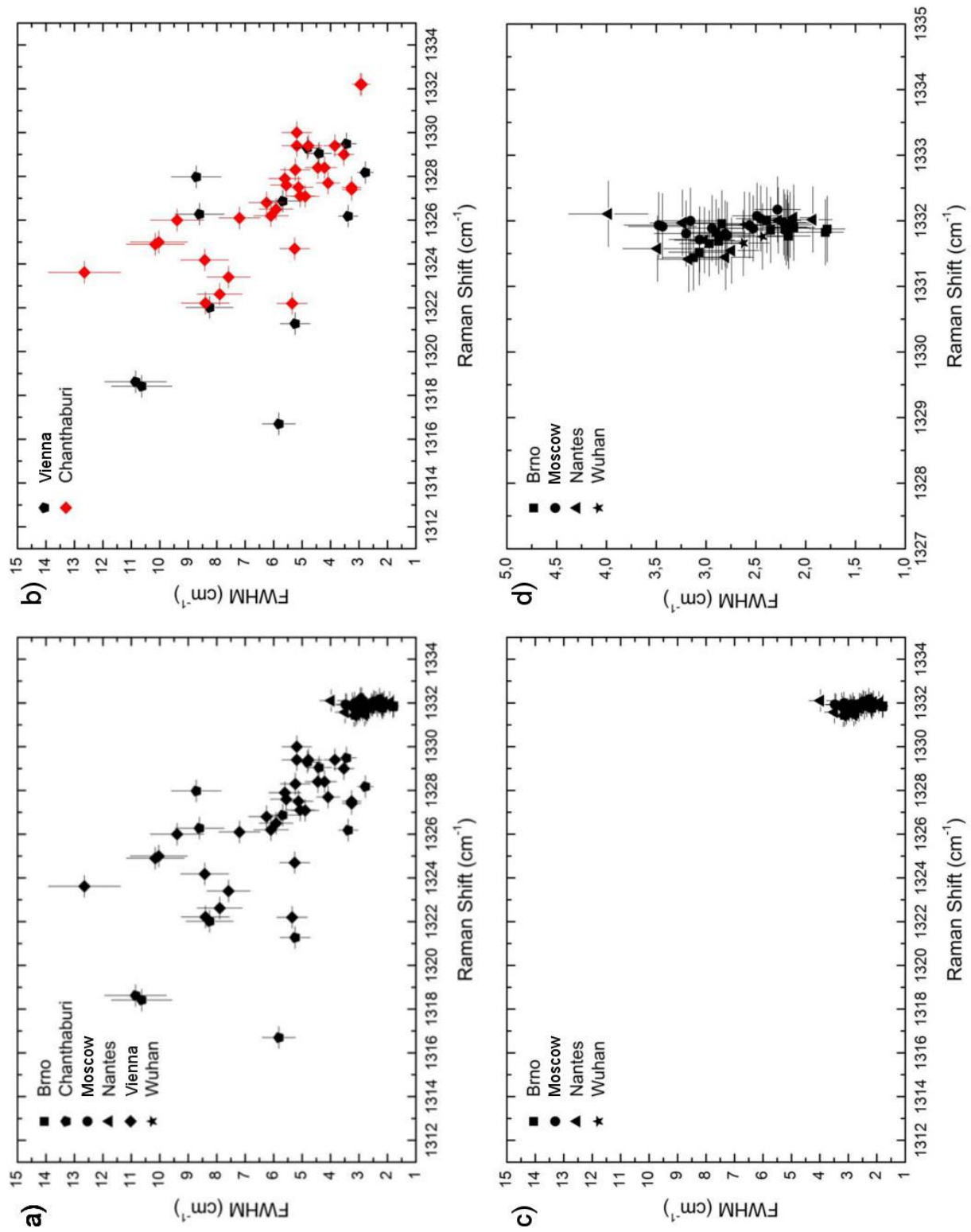


Fig.17 Plot of FWHM against Raman shift of the main diamond Raman band for a) all abrasives b) abrasive samples from the laboratories in Vienna and Chanthaburi c) all abrasives exclusive those from Vienna and Chanthaburi d) different scaling of c). All measurements were taken with He-Ne 632.8 nm excitation, except the abrasives from Moscow and Vienna which were measured with 532 nm excitation.

The precise origin of the diamond in the Chanthaburi samples is unknown. We merely got the information that these abrasives are sold by a local Thai vendor who most likely imported the diamond from China. As discussed in chapter 3.2 different reasons for a variation of the Raman parameters as seen above are possible. Since all measurements were taken under controlled environmental conditions, changes caused by temperature variations can be excluded.

Possible reasons for the varying Raman parameters are a very high ^{13}C concentration, radiation damage, tensile stressor artefacts caused by grain size. Since similar spectral trends were observed for the Vienna and Chanthaburi samples, and the manufacturer of the Vienna samples stated explicitly that their abrasives are affected appreciably by stress, the assumption appears worthwhile that spectral changes of the Chanthaburi samples are due to elevated levels of stress, also. Contrariwise, the other abrasives did not yield unusually low Raman shifts and high FWHMs. It may therefore be assumed that those samples have not been stressed on purpose.

5.2 Natural UHP microdiamond

Two different types of samples from the Kokchetav Massif have been measured. First, microdiamond grains that were still completely included in the host mineral, and second, separated diamond crystals. Possible band-position and FWHM changes due to the varied state of the samples were investigated (Fig.16b). The excavated Kokchetav diamond shows a slightly lower Raman shift than the in-situ crystals, but due to the very low differences, it is not possible to tell, whether such a variation is caused by tensile stress.

Being completely included in their host mineral, the diamond samples from the Kokchetav Massif, the Rhodope Mountains and the Saldenbach reservoir can be characterised without a doubt to be of natural origin and not an artefact from the polishing process. Those diamond crystals show a small decrease of the Raman shift ($1329.6\text{--}1332.7\text{ cm}^{-1}$). On the other hand, the samples from Ceuta (which have not been completely embedded, but on the surface) show a stronger trend (Raman shift: $1324.6\text{--}1332.7\text{ cm}^{-1}$, FWHM: $1.7\text{--}4.6\text{ cm}^{-1}$) (Fig.18a,b). A comparison of the Raman parameters of all natural samples with the parame-

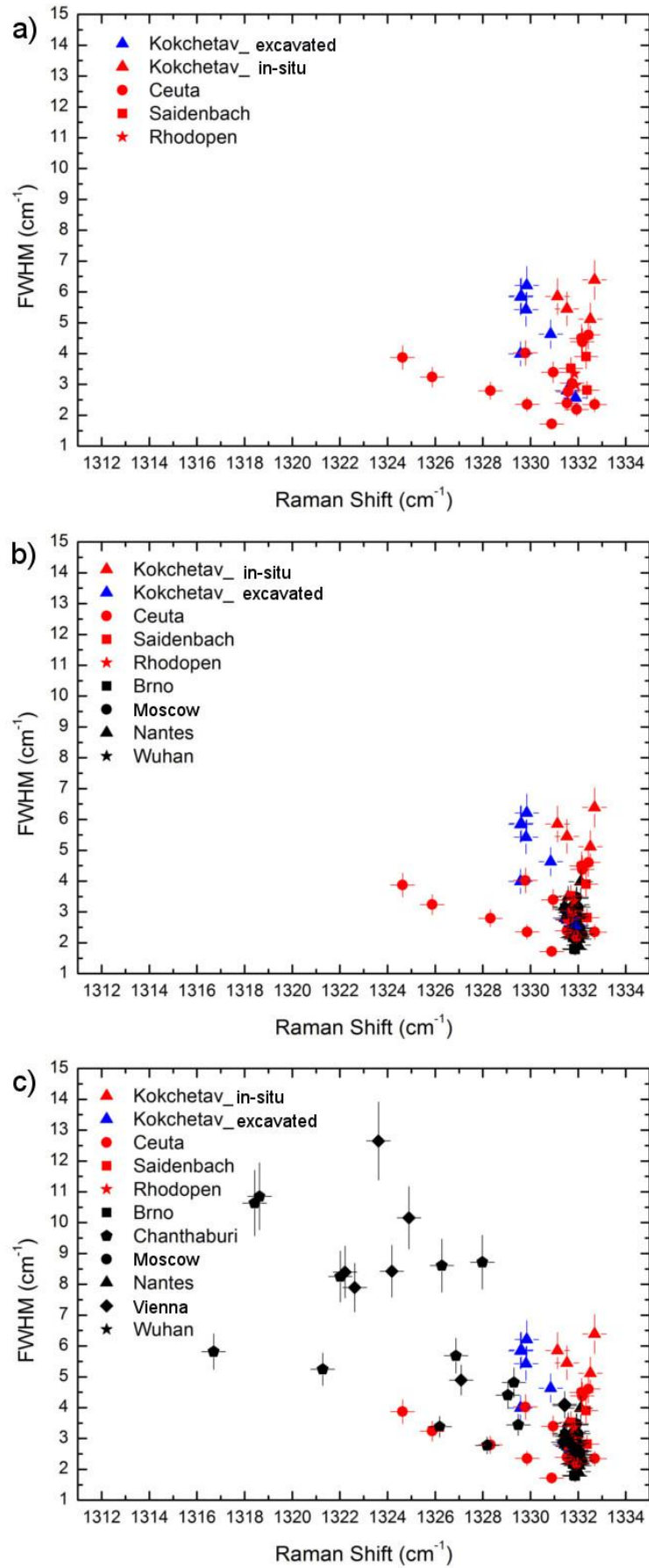


Fig.18 Plot of FWHM against Raman shift of the main diamond Raman band, for a) all natural samples. b) all samples exclusive Vienna and Chanthaburi. c) all measured samples. Red = natural diamond samples, in-situ; blue = natural diamond, separated; black = abrasives.

ters of the abrasives shows that the sample from Ceuta yields different Raman shifts than the other natural diamond samples. However, the decrease of the Raman shifts of the diamond sample from Ceuta is not as strong as the variation by the abrasives from Vienna and Chanthaburi (Fig.18c). According to Ruiz-Cruz & Sanz de Galdeano (2012) the thin sections have been polished using SiC powder to avoid contamination by diamond, though it is not stated whether diamond-based tools were used during the earlier preparation process (i.e. saws, ...). It is therefore not possible to unambiguously identify the microdiamond in the thin sections from Ceuta as natural UHP microdiamond.

The main intention of the present MSc research project was to check critically as to which degree Raman-spectroscopic results might provide the possibility to differentiate between naturally formed diamond and diamond artefacts originating from the preparation process. The results presented here show that the unbiased differentiation of UHP-microdiamond and remnants of diamond abrasives is not possible. Even though some abrasive materials were found to show a very strong decrease in their Raman shift, which was not observed from the four natural samples studied here (and hence could be a distinguishing parameter), spectral trends of UHP microdiamond and abrasives show a wide overlap. Of course reference analyses of the abrasive(s) used may give a hint if unknowns show yielded appreciably deviating parameters. Doubts however cannot be ruled out by Raman measurements alone. Generally, the differentiation between UHP-microdiamond and artefact diamond should be made by means of a multitude of features (see for instance discussion by Perraki et al. 2009). The most reliable supporting feature of natural UHP origin of a diamond would be if euhedral microdiamond is completely included in its host mineral, i.e. still located below the sample surface and not adjacent to a fracture. In contrast, a rather shapeless diamond protruding to the surface or located in or near a fracture could easily be the result of contamination. Such individuals should be examined with great caution.

6. Appendices

Appendix I: Data table

Table 3 FWHM and Raman shift of diamond-based abrasives.

Sample	Grain size [μm]	FWHM [cm^{-1}]	Raman shift [cm^{-1}]
Brno	1	3.32	1331.44
Brno	1	3.09	1331.69
Brno	1	3.18	1331.65
Brno	1	3.27	1331.52
Brno	3	3.11	1331.82
Brno	3	2.45	1331.77
Brno	3	2.61	1331.86
Brno	3	2.48	1331.91
Brno	3	3.06	1331.96
Brno	5	2.40	1331.90
Brno	5	2.64	1332.01
Brno	5	2.11	1331.88
Brno	5	2.13	1331.83
Chanthaburi	0-3	4.55	1329.05
Chanthaburi	0-3	8.79	1327.98
Chanthaburi	0-3	8.68	1326.28
Chanthaburi	0-3	5.79	1326.87
Chanthaburi	0-3	4.95	1329.30
Chanthaburi	0-5	8.33	1322.02
Chanthaburi	0-5	3.00	1328.18
Chanthaburi	0-5	3.56	1326.19
Chanthaburi	0-5	5.37	1321.28
Chanthaburi	0-5	5.93	1316.70
Chanthaburi	0-5	10.91	1318.62
Chanthaburi	0-5	10.70	1318.42
Chanthaburi	0-5	3.63	1329.49
Moscow	1	3.62	1331.91
Moscow	1	3.15	1331.89
Moscow	1	3.39	1331.81
Moscow	1	3.66	1331.93
Moscow	1	3.27	1331.72
Moscow	3	2.73	1332.08
Moscow	3	3.03	1331.81

Sample	Grain size [μm]	FWHM [cm^{-1}]	Raman shift [cm^{-1}]
Moscow	3	3.01	1331.78
Moscow	3	2.55	1332.17
Moscow	3	2.70	1332.03
Moscow	2-3	2.77	1331.88
Moscow	2-3	3.35	1332.00
Moscow	2-3	2.80	1331.93
Moscow	2-3	2.49	1331.97
Nantes	1	3.37	1331.41
Nantes	1	3.02	1331.45
Nantes	1	2.97	1331.55
Nantes	1	3.67	1331.58
Nantes	3	2.46	1331.97
Nantes	3	3.22	1331.70
Nantes	3	2.24	1332.02
Nantes	3	2.40	1332.05
Nantes	6	2.43	1331.94
Nantes	6	4.14	1332.11
Nantes	6	2.47	1331.82
Nantes	6	2.54	1332.01
Nantes	6	3.43	1331.97
Vienna	0.25	7.98	1322.62
Vienna	0.25	8.50	1324.18
Vienna	0.25	10.22	1324.90
Vienna	0.25	5.02	1327.09
Vienna	0.25	12.70	1323.62
Vienna	0.25	8.47	1322.22
Vienna	1	2.61	1331.92
Vienna	1	2.58	1331.89
Vienna	1	2.58	1332.04
Vienna	1	2.59	1332.06
Vienna	3	4.12	1331.43
Vienna	3	4.06	1331.43
Vienna	3	2.88	1331.37
Vienna	3	2.96	1331.56
Vienna	3	2.75	1331.76
Wuhan	<2	2.68	1331.76
Wuhan	<2	2.46	1331.89
Wuhan	<2	3.06	1331.76
Wuhan	<2	2.85	1331.94
Wuhan	<2	2.86	1331.66

Table 4 FWHM and Raman shift of natural UHP microdiamond samples.

Sample	FWHM [cm^{-1}]	Raman shift [cm^{-1}]
Ceuta	2.61	1332.69
Ceuta	4.52	1332.17
Ceuta	4.74	1332.42
Ceuta	4.64	1332.14
Ceuta	2.06	1330.89
Ceuta	3.02	1328.31
Ceuta	2.64	1331.53
Ceuta	2.61	1329.85
Ceuta	3.43	1325.87
Ceuta	4.03	1324.63
Ceuta	2.46	1331.93
Ceuta	3.25	1331.75
Ceuta	3.58	1330.95
Ceuta	2.98	1331.57
Ceuta	4.18	1329.79
Kokchetav_excavated	5.54	1329.81
Kokchetav_excavated	5.98	1329.60
Kokchetav_excavated	6.31	1329.84
Kokchetav_excavated	3.02	1331.54
Kokchetav_excavated	2.80	1331.88
Kokchetav_excavated	4.77	1330.84
Kokchetav_excavated	5.95	1329.58
Kokchetav_excavated	4.15	1329.58
Kokchetav_in-situ	5.24	1332.51
Kokchetav_in-situ	5.57	1331.53
Kokchetav_in-situ	6.49	1332.68
Kokchetav_in-situ	5.96	1331.13
Kokchetav_in-situ	6.49	1332.68
Rhodopen	3.35	1331.84
Rhodopen	2.98	1331.91
Saidenbach	4.07	1332.33
Saidenbach	3.03	1332.37
Saidenbach	3.70	1331.69

Appendix II: Additional figures

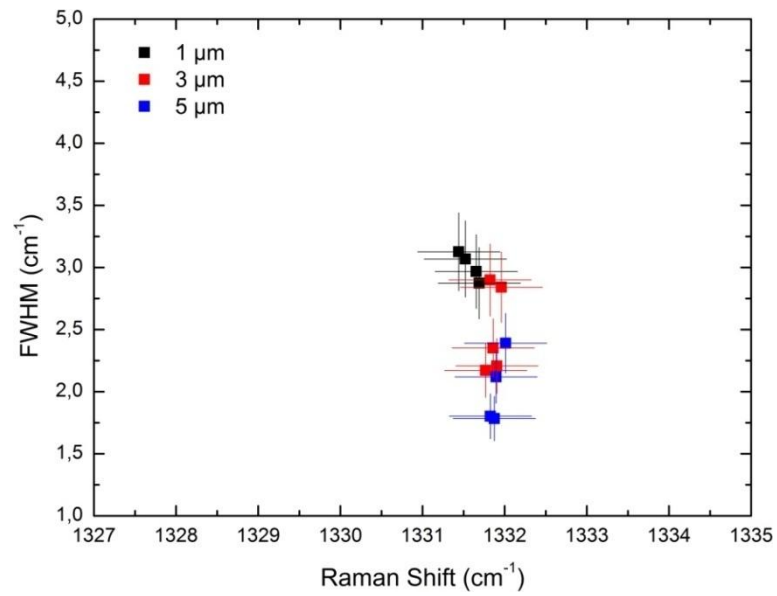


Fig.19 Plot of FWHM against Raman shift of the main diamond Raman band, for abrasives of different grain size from Brno.

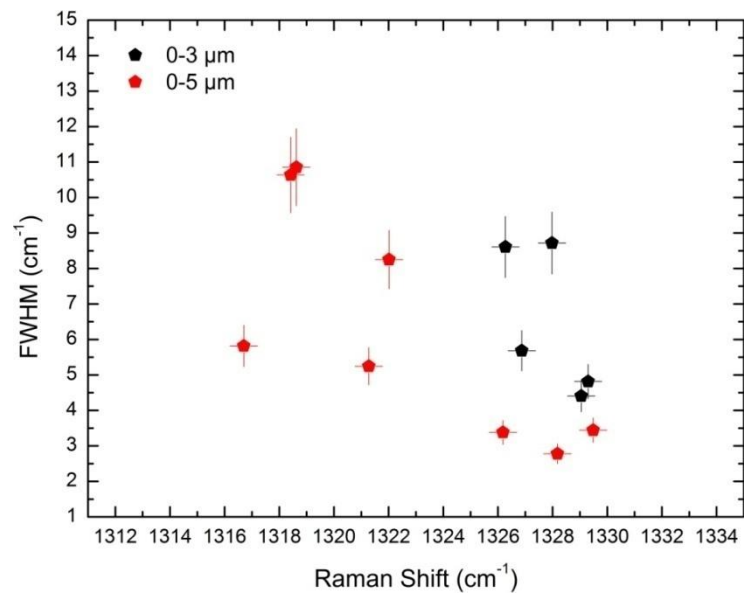


Fig.20 Plot of FWHM against Raman shift of the main diamond Raman band, for abrasives of different grain size from Chanthaburi.

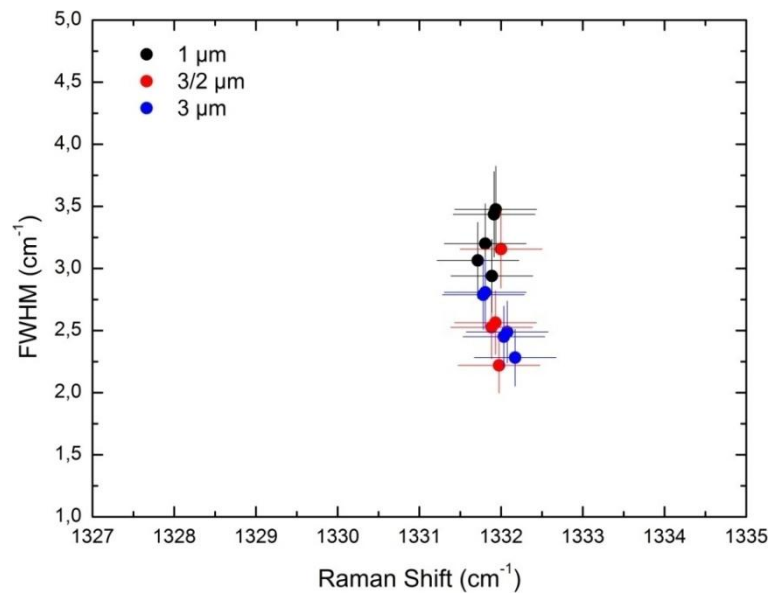


Fig.21 Plot of FWHM against Raman shift of the main diamond Raman band, for abrasives of different grain size from Moscow.

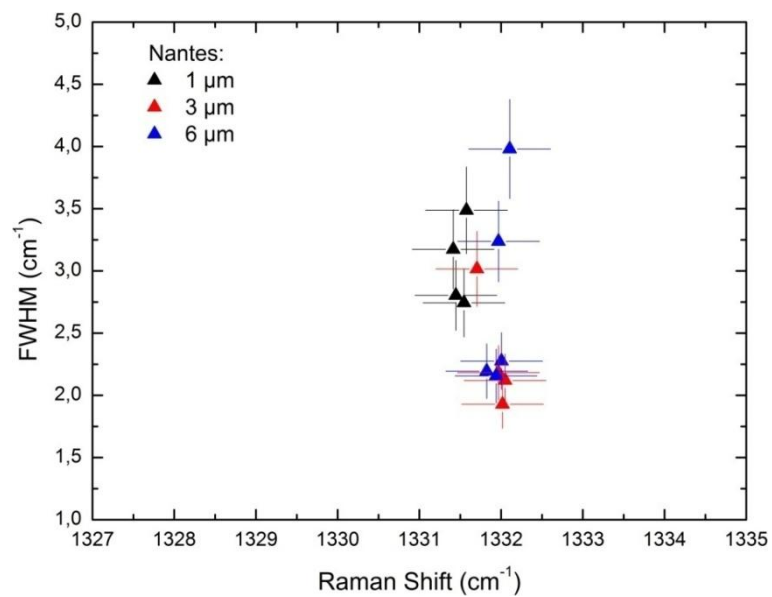


Fig.22 Plot of FWHM against Raman shift of the main diamond Raman band, for abrasives of different grain size from Nantes.

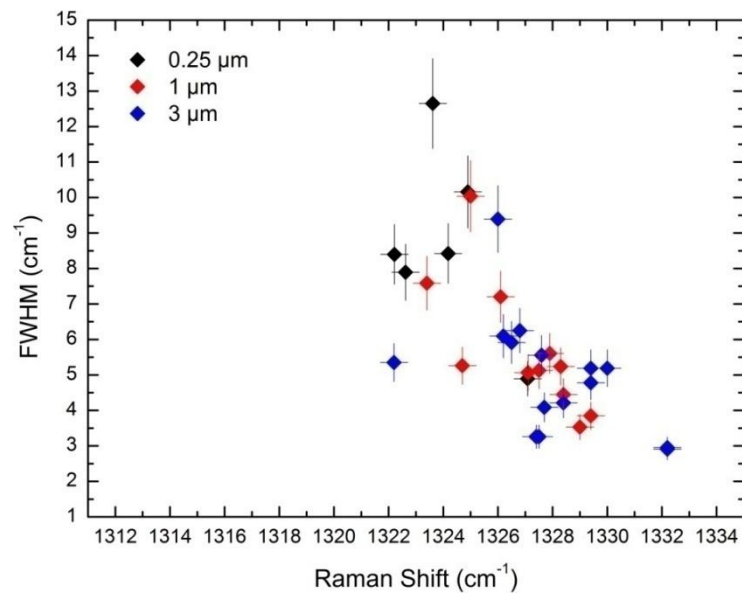


Fig.23 Plot of FWHM against Raman shift of the main diamond Raman band, for abrasives of different grain size from Vienna.

Appendix III: List of Figures

Fig.1 Comparison of Raman shift and bandwidth of diamond samples (image from Menneken et al. 2007)	13
Fig.2 Plots of Raman spectral parameters of the main diamond band. (a) Two diamond-based MRB abrasives (Resin bond diamond powder, Mant USA, Inc.; open symbols = fresh powders; full symbols = used powders). (b) UHP microdiamond (full symbols = present work; open symbols = data from Menneken et al. 2007 and Perraki et al. 2009; ▽▼ = Saidenbach, Erzgebirge, Germany; □ = Jack Hills, Western Australia; ○ = Rhodopes, Greece; ☆ = Kokchetav, Northern Kazakhstan). (from Steger et al. 2013)	14
Fig.3 Elucidation of the light-molecule interaction using a simplified energy level diagram. (1) Infrared absorption. (2) Rayleigh scattering (3) Raman scattering with (3a) Stokes type and (3b) anti-Stokes type (Nasdala et al. 2004).	16
Fig.4 Phase diagram for carbon, visualising the stability fields of graphite (α -C) and diamond (β -C). Point E (900°C, ~40 kbar) marks the minimum pressure and temperature conditions needed for the transformation of graphite to diamond. They correspond to a theoretical depth of about 140 km below the Earth's surface (from Ernst 1976; modified).	19
Fig.5 Raman spectrum of an unstressed diamond. Raman shift: 1332.6 cm^{-1} ; FWHM: 2.3 cm^{-1}	21
Fig.6 Polishing paste samples on object slides. The city names show the location of the laboratories that sent the samples (note that these locations do not correspond to the manufacturing origin). The numbers show the grain size in μm , respectively the product name (Canberra)	24
Fig.7 Back scattered electron microscopy (BSE) image of the Brno abrasive (grain size: 5 μm)	25
Fig.8 BSE image of the Chanthaburi abrasive (grain size: 0–5 μm)	26
Fig.9 BSE image of the Moscow abrasives a) from the company Buehler (grain size: 3 μm) b) from a local Russian manufacturer (grain size: 2–3 μm)	27
Fig.10 BSE image of the Nantes abrasive (grain size: 6 μm).	28
Fig.11 BSE image of the abrasive from Vienna (grain size: 3 μm)	29

Fig.12 Reflected-light image of an assumed microdiamond (marked with arrow) in garnet, from Ceuta, Spain.	31
Fig.13 Plane-polarised transmitted-light microphotograph of a garnet from the Kokchetav Massif. The microdiamond is marked with an arrow.	32
Fig.14 Reflected-light image of a thin section from the Rhodope Mountains, Greece.	32
Fig.15 Plane-polarised transmitted-light image of diamond inclusions in a zircon grain from the Saidenbach reservoir, Germany. Note the focus is well beneath the polished sample surface.	33
Fig.16a) Plot of FWHM against Raman shift of the main diamond Raman band, for abrasives of different grain size from Nantes. b) Analogous plot for two samples of natural UHP diamond from the Kokchetav Massif. All measurements were taken with He-Ne 632.8 nm excitation.	34
Fig.17 Plot of FWHM against Raman shift of the main diamond Raman band for a) all abrasives b) abrasive samples from the laboratories in Vienna and Chanthaburi c) all abrasives exclusive those from Vienna and Chanthaburi d) different scaling of c). All measurements were taken with He-Ne 632.8 nm excitation, except the abrasives from Moscow and Vienna which were measured with 532 nm excitation.	36
Fig.18 Plot of FWHM against Raman shift of the main diamond Raman band, for a) all natural samples. b) all samples exclusive Vienna and Chanthaburi. c) all measured samples. Red = natural diamond samples, in-situ; blue = natural diamond, separated; black = abrasives.	38
Fig.19 Plot of FWHM against Raman shift of the main diamond Raman band, for abrasives of different grain size from Brno.	43
Fig.20 Plot of FWHM against Raman shift of the main diamond Raman band, for abrasives of different grain size from Chanthaburi.	43
Fig.21 Plot of FWHM against Raman shift of the main diamond Raman band, for abrasives of different grain size from Moscow.	44
Fig.22 Plot of FWHM against Raman shift of the main diamond Raman band, for abrasives of different grain size from Nantes.	44
Fig.23 Plot of FWHM against Raman shift of the main diamond Raman band, for abrasives of different grain size from Vienna.	45

Appendix IV: List of Tables

Table 1 Providers of diamond-based abrasives.	23
Table 2 Providers of UHP microdiamond samples.	30
Table 3 FWHM and Raman shift of diamond-based abrasives.	40
Table 4 FWHM and Raman shift of natural UHP microdiamond samples.	42

Appendix V: References

- Anthony J.W., Bideaux R.A., Bladh K.W., Nichols M.C. Eds. (1990) Handbook of Mineralogy. Mineralogical Society of America, Chantilly VA, 588 p.
- Breeding C.M., & Shigley J.E. (2009) The “Type” classification system of diamonds and its importance in gemology. *Gems Gemol* 45: 96–111
- Dijkman F.G., van der Maas J.H. (1976) Dependence of bandshape and depolarization ratio on slitwidth. *Appl Spectrosc* 30: 545–546
- Dobrzhinetskaya L., Wirth R., Green H. (2014) Diamonds in Earth’s oldest zircons from Jack Hills conglomerate, Australia, are contamination. *Earth Planet Sc Let* 87: 212–218.
- Ernst W.G. (1976) Petrologic phase equilibria. Freeman, San Francisco, 333 p.
- Hass K.C., Tamor M.A. (1992) Lattice dynamics and Raman spectra of isotopically mixed diamond. *Phys Rev B* 45/13: 7171–7182
- Irmer G (1985) Zum Einfluß der Apparatfunktion auf die Bestimmung von Streuquerschnitten und Lebensdauern aus optischen Phononenspektren. *Exp Tech Phys* 33:501-506
- Jamieson D.N., Prawer S., Nugent K.W., Dooley S.P. (1995) Cross-sectional Raman microscopy of MeV implanted diamond. *Nucl Instrum Methods B* 106: 641–645
- Kaneko Y., Maruyama S., Terabayashi M., Yamamoto H., Ishikawa M., Anma R., Parkinson C.D., Ota T., Nakajima Y., Katayama I., Yamamoto J., Yamauchi K. (2000) Geology of the Kokchetav UHP-HP metamorphic belt, Northern Kazakhstan. *Isl Arc* 9: 264–283

- Knight D.S., White W.B. (1989) Characterization of diamond films by Raman spectroscopy. *J Mater Res* 4/2: 385–393
- Koivula J.I. (2000) The microworld of diamonds. Gemworld International, Inc., Northbrook, 157 p.
- Massonne H.-J. (2003) A comparison of the evolution of diamondiferous quartz-rich rocks from the Saxonian Erzgebirge and the Kokchetav Massif: are so-called diamondiferous gneisses magmatic rocks?. *Earth Planet Sc Lett* 216: 347–364
- Menneken M., Nemchin A.A., Geisler T., Pidgeon R.T., Wilde S.A. (2007) Hadean diamonds in zircon from Jack Hills, Western Australia. *Nature* 448: 917–921
- Nasdala L., Massonne H.-J. (2000) Microdiamonds from the Saxonian Erzgebirge, Germany: in situ micro-Raman characterisation. *Eur J Mineral* 12: 495–498
- Nasdala L., Brenker F.E., Glöckner J., Hofmeister W., Gasparik T., Harris J.W., Stachel T., Reese, I., (2003) Spectroscopic 2D-tomography: Residual pressure and strain around mineral inclusions in diamonds. *Eur J Mineral* 15: 931–935.
- Nasdala L., Smith D. C., Kaindl R., Ziemann M. A., (2004) Raman spectroscopy: Analytical perspectives in mineralogical research. In: Beran A, Libowitzky E, Eds., *Spectroscopic methods in mineralogy*, Eur Mineral Union Notes in Mineralogy, vol 6. Eötvös Univ Press, Budapest, pp 281–343
- Pearson D.G., Brenker F.E., Nestola F., McNeill J., Nasdala L., Hutchison M.T., Matveev S., Mather K., Silversmit G., Schmitz S., Vekemans B., Vincze L., (2014) Hydrous mantle transition zone indicated by ringwoodite included within diamond. *Nature* 507: 221-224.
- Perraki M., Korsakov A.V., Smith D.C., Mposkos E. (2009) Raman spectroscopic and microscopic criteria for the distinction of microdiamonds in ultrahigh-pressure metamorphic rocks from diamonds in sample preparation materials. *Am Mineral* 84: 546–556
- Ruiz-Cruz M.D., Sanz de Galdeano C. (2012) Diamond and coesite in ultrahigh-pressure–ultrahigh-temperature granulites from Ceuta, Northern Rif, northwest Africa. *Mineral Mag* 76/3: 683–705

- Sauer R. (1999) Synthetic Diamond - Basic Research and Applications. Cryst Res Technol 34: 227-241
- Schertl H.-P., Sobolev N.V. (2012) The Kokchetav Massif, Kazakhstan: "Type locality" of diamond-bearing UHP metamorphic rocks. J Asian Earth Sci 63: 5–38
- Schmidt S., Nagel T.J., Froitzheim N. (2010) A new occurrence of microdiamond-bearing metamorphic rocks, SW Rhodopes, Greece. Eur J Mineral 22: 189–198
- Sharma S.K., Mao H.K., Bell P.M., Xu J.A. (1985) Measurement of Stress in Diamond Anvils with Micro-Raman Spectroscopy. J Raman Spectrosc 18/5: 350–352
- Smith D.C. (1984) Coesite in clinopyroxene in the Caledonides and its implications for geodynamics. Nature 310: 641–644
- Sobolev N.V., Shatsky V.S. (1990) Diamond inclusions in garnets from metamorphic rocks: a new environment for diamond formation. Nature 343: 742–746
- Solin S.A., Ramdas A.K. (1970) Raman spectrum of diamond. Phys Rev B 1/4: 1687–1698
- Steger S., Nasdala L., Wagner A. (2013) Raman spectra of diamond abrasives and possible artefacts in detecting UHP microdiamond. CORALS–2013, Wien, Austria, July, 2013. Book of abstracts, pp. 95–96
- Tanabe K. & Hiraishi J. (1980) Correction of finite slit width effects on Raman line widths. Spectrochim Acta A 36: 341–344
- Mant USA, Inc., <http://www.mantusa.com/powders.htm>, 13.9.2014

Appendix VI: Curriculum vitae

Personal Data

Name Claudia Reissner

Education

June 2008 **Graduation** at the Wiedner Gymnasium - Sir-Karl-Popper-Schule for gifted students

Oct 2008 - Feb 2009 Studies of **Technical Mathematics** at the Technical University of Vienna

Since March 2009 Studies of **Earth Sciences** (focus on Mineralogy and Crystallography) at the University of Vienna

September 2013 **Bachelor of Science**, Bachelor thesis: Orientation dependences of rare earth element emissions in photoluminescence spectra, supervised by Prof. Lutz Nasdala

Working Experience

July 2009 Employment at the **ICAME2009** [International Conference on the Applications of the Mössbauer Effect] at the Technical University of Vienna

Feb - Oct 2011 Temporal employment for a **project** on the manufacturing and dyeing of artificial granite at the Institute of Mineralogy and Crystallography, University of Vienna

Mar - Jun, 2011-2014 **Tutor** at the mineralogical laboratory course

Additional Skills

2002	Seminar on team competence and conflict management
2003	Seminar on presentation techniques
2004-2008	Course on Communication and Social Competence (2 hours a week)
2005	Seminar on rhetoric and presentation
2005	English course at the Studio School of English, Cambridge
2014	Course on blasting engineering at the Technical University of Vienna

Publications

Reissner C., Lenz C., Nasdala L. (2013) Orientation dependences of rare earth element emissions in photoluminescence spectra. CORALS–2013, Wien, Austria, July, 2013. Book of abstracts, pp. 87–88

Knowledge of Data Processing

Microsoft Office, Origin, NGS LabSpec, PeakFit, MatLab, GIMP, CorelDraw, Photoshop

